Important Role of Thermal Inertia for Urban Heat Island Circulation Dynamics

Masanori Onishi[1], Isao Iizawa[2], Miki Fukuzawa[3], Satoshi Sakai[4], Kazuhiro Umetani[5], Aya Ito[6], Arata Yajima[7], Kosaku Ono[8], Naoki Amemura[9]

[1] *Kobe University, 1-1, Rokkodai-cho, Nada-ku, Kobe, Hyogo, Japan, onishi@gfd-dennou.org*
[2] *Kyoto Municipal Horikawa High School, Japan, i.iizawa@gmail.com*
[3] *Kyoto University, Japan, mikimiki.f@outlook.com*
[4] *Kyoto University, Japan, sakai@gaia.h.kyoto-u.ac.jp*
[5] *Okayama University, Japan, umetani@okayama-u.ac.jp*
[6] *Kyoto University, Japan, sonata_no14_in_c_sharp_minor@yahoo.co.jp*
[7] *Tokyo Tatemono Co., Ltd, Japan, aratayaji@yahoo.co.jp*
[8] *Kyoto City, Japan, ko.ono@suido.city.kyoto.jp*
[9] *Kobe College Junior and Senior High School, Japan, amemura@kobejogakuin-h.ed.jp*

1. Introduction

The urban heat island is having been one of important research objects of urban climatology and atmosphere dynamics since the first evidence provided by Howard (1833). In studies on urban climatology, urban heat island has been observed for describing its character in many cities in various sizes, populations, terrains and so on. Heat storage in urban canopy has been considered as important cause of the thermal non-uniformity between urban and rural. In order to establish model of urban canopy layer, heat budget on urban canopy layer has been investigated (e.g. Offerle et al 2005). In the studies of atmosphere dynamics, heat island circulation has been focused. Steady state heat island circulation regime has been studied using a liner theory (Stommel and Veronis 1957, Kimura 1975), numerical simulation (Olfe and Lee 1971), or a laboratory experiment (Kimura 1975). A formation process of heat island circulation and flow regime were studied by a nonlinear theory (Mori and Niino 2002).

Haeger-Eugensson and Holmer (1999) showed that thermal advection was generated at night by thermal ununiformity derived urban heat island. This suggests the difference of temperature between urban and rural observed by us is decided by a result of self-regulation of urban heat island and heat island circulation. In the previous works the temperature of air or surface of ground was used for estimating thermal inertia and anthropogenic heat by observation. As previously described, the temperature was under the effect of thermal transport of heat island circulation.

Therefore, in order to improve the integrated comprehension of the urban heat island, it is needed to estimate effects to urban heat island by thermal inertia, anthropogenic heat and heat island circulation. It is, however, difficult to estimate each effect by factors unless they are investigated all together. The observed urban heat island is under the effect of an interaction that the convection generated by urban heat island alleviates thermal non-uniformity. To separate the effect of self-regulation by heat island circulation from intensity of urban heat island, we need to measure a thermal response of the area on enough short time-scale not to be influenced by the effect of the thermal advection. Therefore observation of urban heat island with high resolution in time is needed to be carried out.

2. Method

2.1 Study area and site description

Kyoto is located in a basin, surrounded on north, east and west sides the by mountains on the central-western part of the island of Honshu (135’ 46’’ N; 35’ 00’’E). Kyoto has a population of 1.5 million. Built-up area lays center of basin. Southern area of basin is covered in fields of rice within 8km radius.

37 sites were selected in study area to figure a lattice network covering urban and rural area. Sites were named as figure 1; alphabet character used from the west toward the east, the number used form north toward south. Figure 1 also shows land-use of Kyoto. In this study, C7 and C2 were defined as be representative site of urban area and rural area.

2.2 Instrumentation and measurements

For this observation we used instruments developed by Umetani (2007); thermometers, long-wave radiation meters and data loggers. Thermistor thermometer (103JT-050, produced by Ishizuka Electronics Corporation) with radiation shield was used for temperature measurement instrument. It has a margin of error of 0.3 deg C. A

radiation thermometer was used as long-wave radiation meter. The mean long-wave radiance from the whole hemisphere is equals to the radiance from 'representative zenith angle' which has a value of 52.5 degree (Dalrymple and Unsworth 1978). We measured the radiation from representative zenith angle by the radiation thermopile (15TP551N, produced by Ishizuka Electronics Corporation). This long-wave radiation meter shows net upward radiant flux assuming that air temperature is equivalent to the surface temperature. This sensor is able to be used as a cloud sensor. When clouds appear net upward radiation is decrease because the bottom of cloud emits more intense long-wave radiation than clear sky. The detail of sensor is described in Sakai et al., (2009).

The data was gathered using electronic data loggers. The loggers were special designed for high accuracy observation. They have 6-channel 12-bit A/D converter and 1M memory, can record 2 channel data for about 2 weeks on the minute.

Those instruments were settled on north-side of trees lining a street for preventing as much of effect of direct sunlight as possible (Fig 2). The thermistor thermometer was settled at level of 1.5m height from the ground. The radiation thermometer was directed to a zenith angle of 52.5 degree.

The logger read the value each the second and recorded average value of each the second per 1 or 2 minute(s).

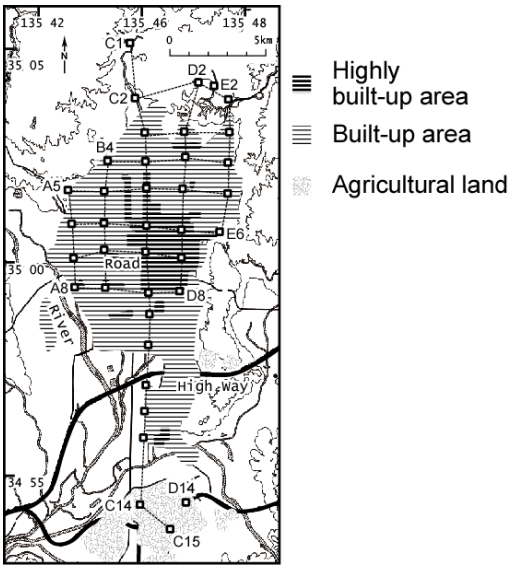

Fig. 1 Map of observation sites.

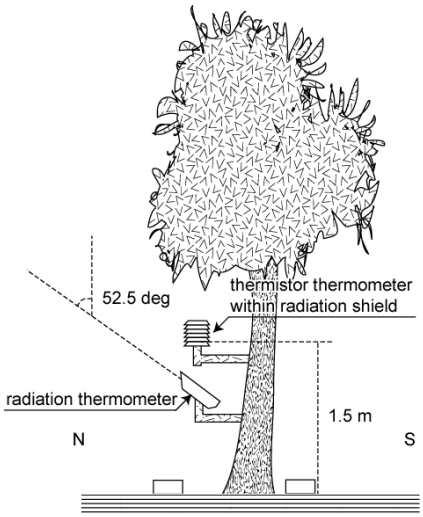

Fig. 2 Schematic of installation condition of instruments.

2.3 Observation

We conducted observations of 8 periods once every season during the 2004-2006. List of observation periods and number of sites is shown Table 1.

Observation periods	Number of temperature sites	Number of radiation sites
3-7 Nov. 2004	24	0
28 Feb-12 Mar. 2005	35	8
13-24 May. 2005	36	12
10-26 Aug. 2005	36	16
10-23 Oct. 2005	36	17
19 Jan. – 12 Feb. 2006	19	19
24 Apr. – 7 May. 2006	19	19
24 Jul-6 Aug. 2006	19	19

Table 1 List of observation periods and number of observation sites

2.4 Estimation of effective thermal inertia

The temperature *T* decreased by only downward net long-wave radiant flux *R* which is generally negative during night, is given as

$$T = T_{sunset} + \frac{2}{\sqrt{\rho}}\frac{R}{I}\sqrt{t} \quad (1)$$

, where T_{sunset} is temperature at sunset, *I* is sum of thermal inertia of surface material and *t* is elapsed time (Brunt, 1942). Here we consider that the downward radiant flux instantly increases, for example it becomes suddenly cloudy. In this case, a cooling rate of air temperature is decrease. Assuming heating by the radiant flux suddenly increased is divided into a heating by increased downward radiant flux $\triangle R$ and the downward radiant flux before increased, a heating rate after the flux changed is expressed as

$$T = T_{sunset} + \frac{2}{\sqrt{\rho}}\frac{R}{I}\sqrt{t} + \frac{2}{\sqrt{\rho}}\frac{\Delta R}{I}\sqrt{t - t_0} \quad (2)$$

, where t_0 is the time at flux changed. When $(t - t_0) / t_0 \ll 1$, Eq. (2) is approximately expressed as

$$T = T_0 + \frac{2}{\sqrt{\rho}}\frac{R}{I\sqrt{t_0}}(t - t_0) + \frac{2}{\sqrt{\rho}}\frac{\Delta R}{I}\sqrt{t - t_0} \quad (3)$$

, where T_0 is the temperature at $t=t_0$.

Defining a hypothetical temperature of case that flux remain *T'* is as

$$T' = T_0 + \frac{2}{\sqrt{\rho}}\frac{R}{I\sqrt{t_0}}(t - t_0). \quad (4)$$

The difference of temperature $\triangle T_R$ between *T* and *T'* is expressed as

$$\Delta T_R = \frac{2}{\sqrt{\rho}}\frac{\Delta R}{I}\sqrt{t - t_0}, \quad (5)$$

using eqs. (3) and (4).
Therefore the thermal inertia is written as follows:

$$I = \frac{2}{\sqrt{\rho}}\frac{\Delta R}{\Delta T_R}\sqrt{t - t_0}. \quad (6)$$

In this study, LETI which does not include the effect of thermal advection was focused. To ignore the effect of thermal advection, elapsed time *t* is needed to be enough small. We decide this time length to 30 minutes in order to focus the area having 1-2km radius because during night a wind speed is at less than 2m/s in generally.

Time series of air temperature and radiant flux was obtained from observation in order to estimate LETI using relation shown in eq. (6). The event at which it suddenly changed to cloudy from cleared sky during nighttime was selected from the observational data by finding radiant flux is suddenly changed.

T' was decided by linear approximation near $t=t_0$,

$$T' = T_0 + k(t - t_0) \quad (7)$$

,where *k* is ratio of *T'* to elapsed time.

$$\Delta T_R = T - T_0 - k(t - t_0). \quad (8)$$

We adopted coefficient of linear approximation of the time series of the temperature at 30 minutes before flux had changed as *k* in eq. (8). *T* was calculated by coefficient of linear approximation of the time series of the temperature at 30 minutes after flux had changed instead of using directly. Change of radiant flax is obtained by averaging some sites near the site of temperature analyzed.

3. Results

3.1 Air temperature

Figure 3 shows air temperature and cooling rate from 15:00 7th to 6:00 8th March 2005. Air temperatures in daytime are almost the same among different observation sites. In nighttime, on the other hand, temperatures in urban and rural sites are different. When air temperatures in those sites begin to be different, cooling rate of rural site reaches a maximum. The times in maximum cooling rate of those sites is earlier in northern sites than in southern sites.

Figure 4 shows spatial distribution of air temperature at a few hours after sunset. Typical air temperature distribution in urban heat island appears in Fig 4.

Figure 5 shows diurnal cycle of temperature difference between urban (C7) and rural (C2) sites. In a few hours after sunset, the temperature difference increases rapidly. Maximum value of the difference is more than 10 degree C. After the maximum value occurs, the temperature difference decreases gradually until sunrise. This diurnal cycle is similar to Haeger-Eugensson & Holmer 1999.

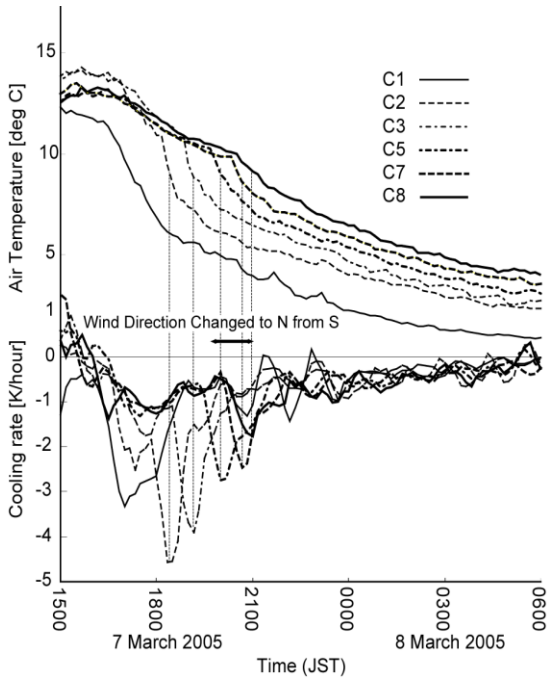

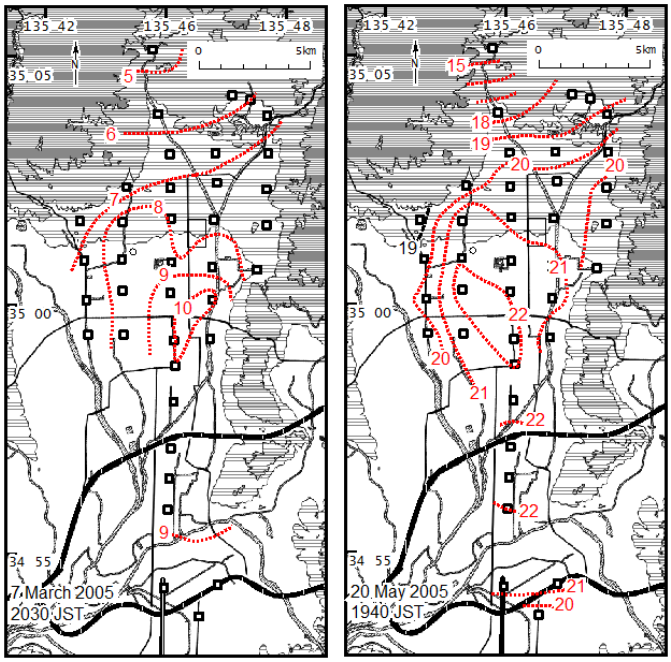

Fig. 3 Time series of the air temperature and cooling rate. *Fig. 4 The spatial distribution of air temperature.*

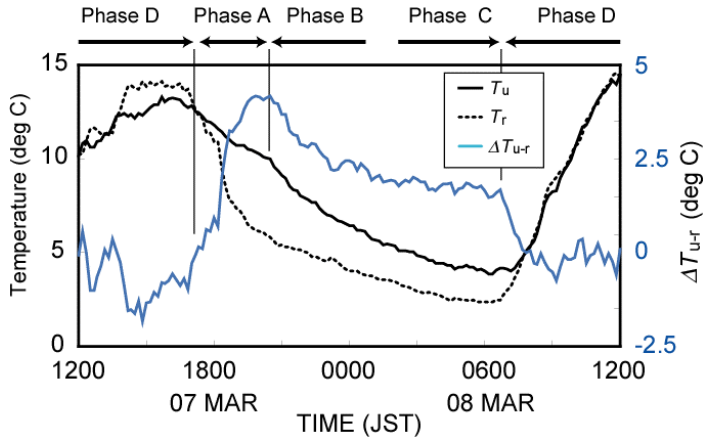

Fig. 5 Time series of air temperature of urban (C7) rural (C2) and the temperature difference between those sites. in 7-8 March 2005.

3.2 Local effective thermal inertia

Table 2 shows local effective thermal inertia in observation sites. The values of LETI in urban area are bigger than those in rural area. In this table, the local effective thermal inertia is shown as average of the estimated value except maximum and minimum. LETI of urban area was estimated as 4.3-7.9×10^3 W/K$s^{1/2}$, of rural area as 1.7-3.4×10^3 W/K$s^{1/2}$. LETI of urban area was more than two times of estimated by the previous works Thermal inertia estimated in previous works would be smaller than real value for temperature decrease by the thermal advection. LETI of urban area was more than two times of the thermal inertia of materials of which urban structure is generally constructed. For using for the wall of a building the material having high thermal inertia LETI of urban seemed to be larger than thermal inertia of the material.

LETI $\times 10^3$ (W/Ks$^{1/2}$) (STDERR)					
Site	A	B	C	D	E
1			3.4 (1.8)		
2			3.3 (1.1)	2.0 (0.6)	2.1 (1.0)
3			3.0 (1.1)	3.3 (0.8)	3.4 (1.5)
4		1.3 (0.5)	3.5 (2.3)	2.9 (0.9)	2.4 (0.5)
5	1.7 (0.8)	2.0 (0.5)	5.6 (4.4)	4.3 (1.8)	3.6 (1.4)
6	2.7 (0.8)	1.6 N/A	4.7 (3.8)	6.2 (2.4)	2.3 (0.6)
7	4.3 (0.5)	6.4 N/A	7.9 (2.5)	6.4 (3.7)	
8	3.0 (1.0)	1.8 N/A	5.6 (1.6)	3.2 (0.5)	
9			4.3 (3.2)		
10			3.6 (5.8)		
11			5.8 (1.5)		
12			3.2 (1.5)		
13			3.2 (3.1)		
14			2.6 (16)	7.2 (1.8)	
15			1.7 (1.5)		

Table 2 List of the local effective thermal inertia.

References

Howard, L., 1833: The Climate of London: Deduced from Meteorological Observations Made in the Metropolis and at Various Places Around it, Harvey and Darton, J. and A. Arch, Longman, Hatchard, S. Highley [and] R. Hunter, 1833

Offerle, B., C. S. B. Grimond and K. Fortunak., 2005: Heat storage and anthropogenic heat flux in relation to the enegy balance of a central european city centre. *Int. J. Climatol.*, **25**, 1450-1419.

Stommel, H., and G. Veronis, 1957: Steady convective motion in a horizontal layer of fluid heated uniformly from above and cooled non-uniformly from below. *Tellus*, **9**, 401–407.

Kimura, R., 1975: Dynamics of steady convections over heat and cool islands. *J. Meteor. Soc. Japan*, **53**, 440–457.

Olfe, D. B., and R. L. Lee, 1971: Linearized calculations of urban heat island convection effects. *J. Atmos. Sci.*, **28**, 1374–1388.

Mori, A. and H. Niino, 2002: Time evolution of nonlinear horizontal convection: Its flow regimes and self-similar solutions. *J. Atmos. Sci.*, **59**, 1841-1856.

Haeger-Eugensson M, Holmer B., 1999: Advection caused by the urban heat island circulation as a regulating factor on the nocturnal urban heat island. *Int. J. Climatol*. **19**, 975–988.

Umetani, K., 2007:. PhD thesis, Kyoto University.

Dalrymple, G. J. and M. H. Unsworth, 1978: Longwave radiation at the ground: IV. Comparison of measurement and calculation of radiation from cloudless skies, *Quart. J. Roy. Meteor. Soc.*, **104**, 989-997.

Sakai et al., 2009: A Practical Pyrgeometer Using the Representative Angle. *Atmos. Oceanic Technol.*, **26**, 647–655.